

Heklaite, KNaSiF_6 , a new fumarolic mineral from Hekla volcano, Iceland

A. GARAVELLI¹, T. BALIĆ-ŽUNIĆ², D. MITOLO¹, P. ACQUAFREDDA¹, E. LEONARSEN³ AND S. P. JAKOBSSON⁴

¹ Dipartimento Geomineralogico, Università di Bari, via E. Orabona 4, I–70125 Bari, Italy

² Department of Geography and Geology, University of Copenhagen, Øster Voldgade 10, DK-1350 København K, Denmark

³ St. Karlsmindevej 46, DK-3390 Hundested, Denmark

⁴ Icelandic Institute of Natural History, Hlemmur 3, P.O. Box 5320, IS-125 Reykjavik, Iceland

[Received 29 January 2010; Accepted 25 March 2010]

ABSTRACT

Heklaite, with the ideal formula KNaSiF_6 , was found among fumarolic encrustations collected in 1992 on the Hekla volcano, Iceland. Heklaite forms a fine-grained mass of micron- to sub-micron-sized crystals intimately associated with malladrite, hieratite and ralstonite. The mineral is colourless, transparent, non-fluorescent, has a vitreous lustre and a white streak. The calculated density is 2.69 g cm^{-3} . An SEM-EDS quantitative chemical analysis shows the following range of concentrations (wt.%): Na 11.61–12.74 (average 11.98), K 17.02–18.97 (average 18.29), Si 13.48–14.17 (average 13.91), F 54.88–56.19 (average 55.66). The empirical chemical formula, calculated on the basis of 9 a.p.f.u., is $\text{Na}_{1.07}\text{K}_{0.96}\text{Si}_{1.01}\text{F}_{5.97}$. X-ray powder diffraction indicates that heklaite is orthorhombic, space group $Pnma$, with the following unit-cell parameters: $a = 9.3387(7) \text{ \AA}$, $b = 5.5032(4) \text{ \AA}$, $c = 9.7957(8) \text{ \AA}$, $V = 503.43(7) \text{ \AA}^3$, $Z = 4$. The eight strongest reflections in the powder diffraction pattern [d in Å (I/I_0) (hkl)] are: 4.33 (53) (102); 4.26 (56) (111); 3.40 (49) (112); 3.37 (47) (202); 3.34 (100) (211); 2.251 (27) (303); 2.050 (52) (123); 2.016 (29) (321). On the basis of chemical analyses and X-ray data, heklaite corresponds to the synthetic compound KNaSiF_6 . The name is for the type locality, the Hekla volcano, Iceland.

KEYWORDS: heklaite, new mineral, sublimates, fumaroles, fluorosilicate, crystal structure, Hekla, Iceland.

Introduction

THE Hekla central volcano, 1491 m in height, is situated on the western border of the Eastern Volcanic Zone in South Iceland (63.59° N , 19.42° W) (Fig. 1) and is one of the most famous volcanoes of the world. It has been active for thousands of years and more than 18 eruptions have been recorded during historical time. Numerous stories were spun from folk beliefs of the terrifying power displayed in Hekla's eruptions, and old stories tell of how

people believed that the souls of the damned passed through the crater of Hekla on their way to Hell. It is often stated that the name given to the volcano in ancient times is derived from the Icelandic word 'hekla', meaning a short hooded cloak which may relate to the frequent cloud cover on the summit or to the patches of snow frequently visible on the top of the mountain.

The last two sizeable eruptions of the Hekla volcano occurred in 1991 and, on a smaller scale, in 2000. The 1991 Hekla eruption started on January 17 with a short-lived Plinian phase which was accompanied with an effusive lava phase (Gudmundsson *et al.*, 1992). After two days of eruption, the volcanic activity was restricted mainly to a single fissure trending east-southeast from the top of the mountain. The eruption came

* E-mail: a.garavelli@geomin.uniba.it
DOI: 10.1180/minmag.2010.074.1.147

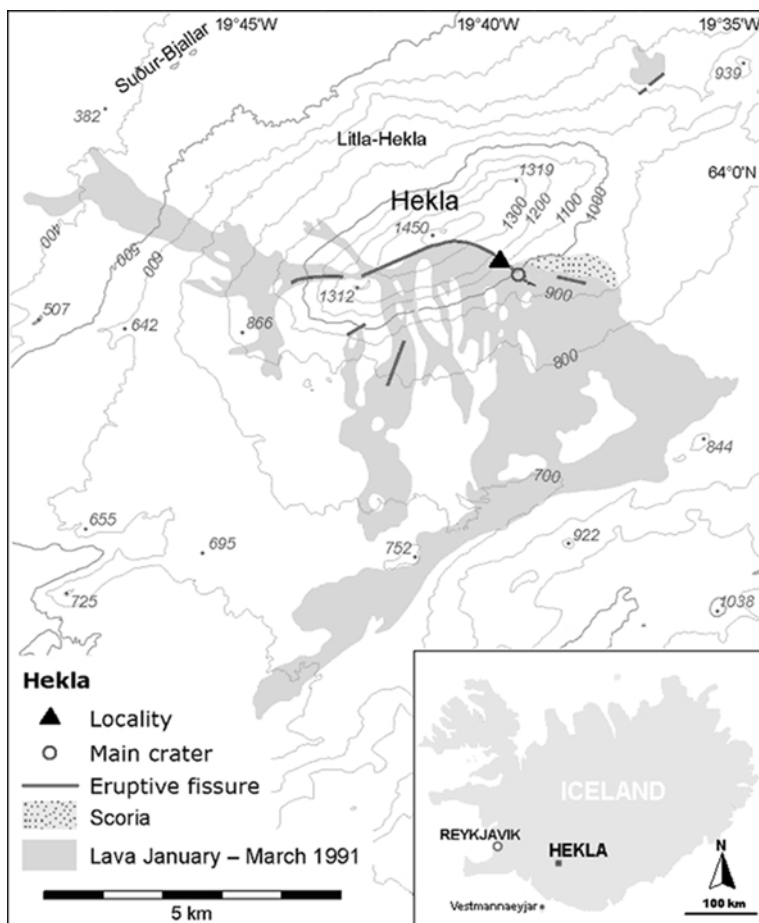


FIG. 1. Eruptive fissures and extrusives of the 1991 Hekla eruption, (modified slightly after Gudmunsson *et al.*, 1992). Heklaite-containing samples were found on the locality shown on the map.

to an end on March 11, 1991. The lava covered about 23 km², and the total amount of tephra and lava produced during the eruption was estimated to be 0.15 km³. The 1991 Hekla extrusives are mugearitic and belong to the transitional alkalic rock series of Iceland; they are characterized by relatively large contents of Fe and F (Jakobsson *et al.*, 2008a). A considerable amount of volcanic gases and vapour was released during the eruption. Pollution of groundwater and rivers around the volcano by F and other elements was observed within a few days of the onset of eruption.

The new mineral described herein, KNaSiF₆, was discovered among sublimes collected after

the 1991 Hekla eruption and is named heklaite after the locality. Taking into account the particular F enrichment in volcanic gases and tephra emitted from Mt. Hekla, the new mineral heklaite rightly bears the name of this volcano. The mineral and its name were approved by the IMA Commission on New Minerals, Nomenclature and Classification (CNMNC) (IMA No 2008-52). The holotype is deposited in the mineral collection of the Icelandic Institute of Natural History, Reykjavik, Iceland, labelled as NI 15513. An additional sample is deposited at the Museum 'C.L. Garavelli', Dipartimento Geomineralogico, Università di Bari, Italy, under the catalogue number 9/nm-V28.

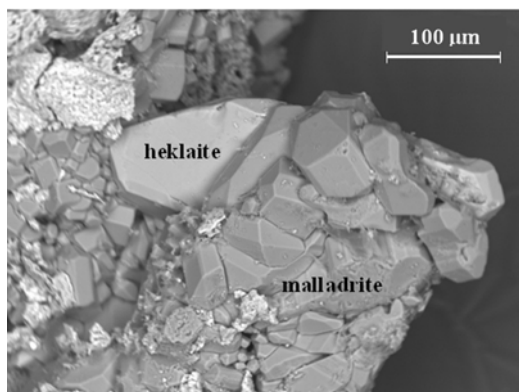


FIG. 2. SEM image of heklaite, KNaSiF_6 , associated with malladrite, Na_2SiF_6 .

Occurrence and physical properties

Hekla volcanic sublimates and encrustations were collected during several sampling expeditions in the period 1991–1993. They were deposited at several localities on the lava and in the main crater (Jakobsson *et al.*, 2008b), but especially around the eruption fissure above the main crater on the northeast side of the mountain, at 1100–1110 m a.s.l. (Fig. 1). Unfortunately, this

locality was subsequently completely covered by scoria produced by the 2000 Hekla eruption.

A recent study of sublimates deposited in the Hekla area after the 1991 eruption (Jakobsson *et al.*, 2008b) indicated the occurrence of 36 different chemical species, 17 of which are potentially new minerals. Heklaite was identified in five different samples collected on September 16, 1992. It was associated with ralstonite [$\text{Na}_x\text{Mg}_x\text{Al}_{2-x}(\text{F},\text{OH})_6 \cdot \text{H}_2\text{O}$], opal-A [$\text{SiO}_2 \cdot n(\text{H}_2\text{O})$], hematite (Fe_2O_3), malladrite (Na_2SiF_6) and three other, possibly new, minerals (Jakobsson *et al.*, 2008b).

Heklaite was collected at gas temperatures as high as 330°C. As the eruption fissure at Hekla was probably cooling slowly and at a steady rate, the measured temperatures at the time of sampling indicate the minimum temperature of deposition of heklaite. In the samples investigated, heklaite forms a fine-grained mass of micrometre- to sub-micrometre-sized crystals typically associated with malladrite and often intimately intergrown with it (Fig. 2). An SEM-EDS investigation indicated that, in some parts of the analysed samples, heklaite is also intergrown with K_2SiF_6 , which is probably the cubic polymorph hieratite, as inferred from its morphology and the fact that hieratite was identified in the X-ray powder diffraction pattern of a sample from the same locality.

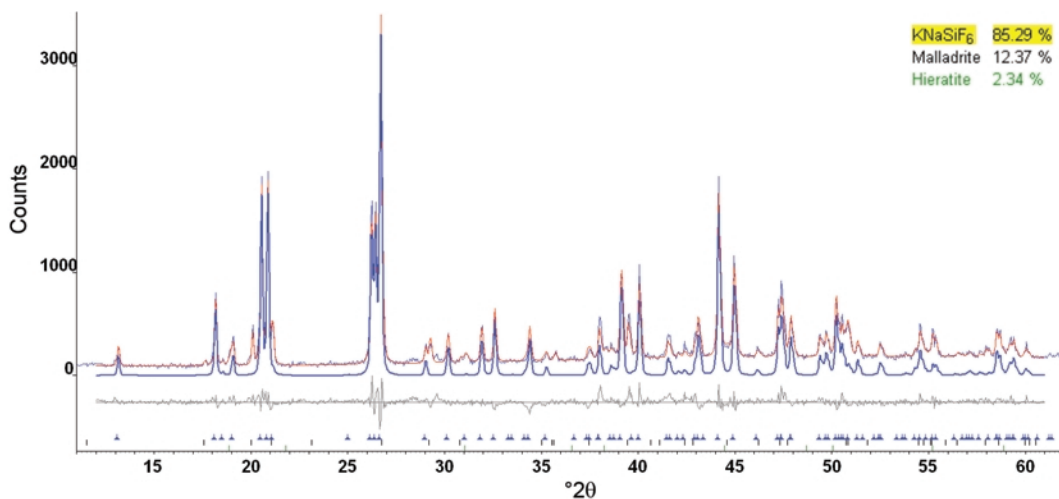


FIG. 3. X-ray powder diffraction diagram of heklaite with minor malladrite and traces of hieratite, with the results of Rietveld refinement. Light blue: experimental diagram, red: calculated diagram, grey: difference, dark blue: calculated pattern of heklaite alone. Marks at the bottom indicate the expected positions of diffraction maxima for heklaite, malladrite and hieratite respectively (from top to the bottom). Bragg-Brentano reflection geometry, $\text{Cu-K}\alpha$ radiation, variable divergence slit.

Heklaite is colourless and transparent, has a white streak, a vitreous lustre and is non-fluorescent in UV light. A quantitative analysis of optical properties could not be carried out due to the small size of the crystals, which also prevented the determination of its hardness. An experimental determination of density was not attempted, because of the intimate admixture with the accompanying minerals. The density, calculated from the empirical formula reported below and the unit-cell data, is 2.69 g cm^{-3} . The powder sample of heklaite and associated minerals remained under laboratory conditions for about four years before its complete definition, and during this time the minerals remained unaltered.

Chemical composition

The electron microscope used for this research was a Cambridge S360 SEM, coupled with an Oxford-Link Ge ISIS energy-dispersive spectrometer equipped with an SATW (Super Atmosphere Thin Window), which permits better detection of the light elements.

Energy-dispersive analysis was chosen for quantitative analysis of the very small crystals instead of a wavelength-dispersive analysis because it allows analysis to be carried out using a lower probe current and a non-critical working distance (Ruste, 1979; Acquafredda and Paglionico, 2004). The use of a lower probe current means that the analysed volume of the crystal becomes critical only if it is smaller than $3 \mu\text{m}$, and this was necessary for our specimens. The non-critical working distance meant that it was possible to obtain quantitative analyses of the heklaite crystals even on slightly tilted, concave or convex, unpolished crystal faces.

The samples were sputtered with a 30 nm-thick carbon film to perform SEM-EDS observations

and microanalysis. The SEM was operated at 15 kV and 500 pA, using 2.5 kcps as an average count rate on the whole spectrum, giving a typical on-peak counting time of 100 s. X-ray counts were converted to wt.% oxides by the ZAF4/FLS quantitative analysis software (Oxford-Link Analytical, UK). The results are reported in Table 1. The empirical formula based on 9 a.p.f.u. is: $\text{Na}_{1.063}\text{K}_{0.954}\text{Si}_{1.010}\text{F}_{5.974}$. The simplified formula is KNaSiF_6 , for which $\text{Na} = 11.26$, $\text{K} = 19.15$, $\text{Si} = 13.76$ and $\text{F} = 55.83 \text{ wt.}\%$, totalling 100.00 wt.%.

Diffraction properties and crystal structure description

X-ray powder diffraction

X-ray powder-diffraction data (XRD) were obtained using a Panalytical (formerly Philips) PW3710 diffractometer with Bragg-Brentano geometry, a long fine-focus X-ray tube with a Cu anode, a secondary graphite monochromator and a variable divergence slit. In the samples studied, heklaite was never pure but always admixed with malladrite and other minerals including ralstonite, hieratite and some, as yet, unidentified phases. A detailed XRD study of the heklaite was carried out on a powder diagram which contained the lowest proportions of the other minerals, in this case about 10 wt.% of malladrite and a few wt.% of hieratite (Fig. 3). The identification of heklaite was based on a comparison with the XRD data for synthetic KNaSiF_6 (PDF 31-1086 and 38-686), whereas the indexing and subsequent Rietveld analysis were based on published crystal structure data for this compound (Fischer and Kraemer, 1991). In Table 2, the XRD data for heklaite and the synthetic analogue are compared. Single-crystal X-ray studies were not attempted because of the

TABLE 1. The results of the chemical analysis (SEM-EDS) of heklaite (average of five point analyses).

Constituent	Wt.%	Range	Std. dev.	Probe standard
Na	11.98	11.61–12.74	0.49	Albite
K	18.29	17.02–18.97	0.88	Orthoclase
Si	13.91	13.48–14.17	0.26	Wollastonite
F	55.66	54.88–56.19	0.50	LiF
Total	99.84	99.01–100.15		

TABLE 2. X-ray powder diffraction data of heklaite compared to synthetic KNaSiF_6 . The eight strongest reflections are given in bold. The reflections of malladrite (*M*) are given in italics.

Heklaite				Synthetic KNaSiF_6 (Fischer and Kramer, 1991)	
l/l_0	$d_{\text{meas.}}$	$d_{\text{calc.}}$	hkl	l/l_0	$d_{\text{meas.}}$
5.4	6.75	6.76	1 0 1	10.3	6.7477
1.5	5.03	5.05	<i>M</i>		
20.1	4.88	4.9	0 0 2	22.9	4.8934
1.5	4.8	4.8	0 1 1	8.7	4.7988
8.9	4.66	4.67	2 0 0		
10.2	4.43	4.43	<i>M</i>		
53.3	4.33	4.34	1 0 2	54.3	4.3331
56.0	4.26	4.27	1 1 1	72.5	4.2642
13.0	4.2	4.22	<i>M</i>		
49.2	3.4	3.41	1 1 2	47.6	3.4037
47.4	3.37	3.38	2 0 2	40.1	3.3753
100.0	3.34	3.35	2 1 1	100.0	3.3424
5.6	3.08	3.08	1 0 3	4.4	3.0796
6.1	3.05	3.06	<i>M</i>		
8.9	2.96	2.97	3 0 1	10.1	2.9625
2.9	2.88	2.88	2 1 2		
11.1	2.8	2.81	0 1 3	9.6	2.8054
13.9	2.75	2.75	0 2 0	11.9	2.7498
7.6	2.61	2.61	3 1 1	6.9	2.6091
2.3	2.55	2.55	1 2 1		
2.5	2.51	2.52	<i>M</i>		
3.3	2.398	2.399	0 2 2		
14.6	2.368	2.369	2 2 0/1 0 4	8.2	2.3674
4.3	2.333	2.334	4 0 0		
26.9	2.301	2.304	2 2 1	16.8	2.3022
14.7	2.281	2.283	<i>M</i>		
27.0	2.251	2.253	3 0 3	14.1	2.2504
8.2	2.172	2.176	1 1 4		
3.4	2.131	2.133	2 2 2		
9.4	2.106	2.107	4 0 2		
10.5	2.099	2.099	4 1 1	6.3	2.0962
51.7	2.050	2.052	1 2 3	28.4	2.0510
28.8	2.016	2.017	3 2 1	17.7 ¹	2.0154
2.4	1.966	1.968	4 1 2		
19.9	1.923	1.924	3 0 4	7.1	1.9234
22.0	1.918	1.918	2 2 3	8.8	1.9155
11.9	1.899	1.900	3 2 2	7.7	1.8978
7.0	1.844	1.845	0 1 5	3.5	1.8439
7.6	1.833	1.834	5 0 1	4.4	1.8323
16.8	1.815	1.817	3 1 4	9.5	1.8148
11.3	1.797	1.795	2 0 5	6.0	1.8058
4.1	1.779	1.780	4 2 0	3.4	1.7780
4.2	1.742	1.743	3 2 3	3.0 ²	1.7421
9.8	1.681	1.682	2 3 1	4.5	1.6806
8.2	1.663	1.663	5 1 2	2.5	1.6616
1.8	1.611	1.611	2 3 2		
3.0	1.589	1.590	<i>M</i>		
9.4	1.575	1.577	3 2 4	4.1	1.5750
5.7	1.558	1.556	3 3 1	2.6	1.5597
3.2	1.540	1.541	2 0 6	3.0	

Plus eight further reflections down to 1.3038 Å

¹ Indexed as 214. However, the dominating reflection is 321.

² Indexed as 502. However, the dominating reflection is 323.

generally small crystal size (the largest observed heklaite crystal shown on Fig. 2 was discovered quite late in this study). Instead, Rietveld refinement (*Topas4*, Bruker-AXS) of the powder pattern was performed in order to confirm the identity of the mineral, its correspondence with synthetic KNaSiF_6 (Fischer and Kraemer, 1991) and to refine its unit-cell parameters. Reliability factors were: $R_{\text{exp}} = 6.17\%$; $R_{\text{wp}} = 10.48\%$; Goodness of Fit = 1.70; $R_{\text{Bragg}} = 6.43\%$, the quantitative phase composition gave the following results: heklaite 85(1) wt.%; malladrite 12(1) wt.%; hieratite 2.3(3) wt.%, and the refined average crystallite size for heklaite was 179(15) nm.

Crystal structure

The crystal structure data are presented in Table 3. Isolated regular SiF_6 octahedra are characteristic of all silicofluorides. In these structures, there is a major difference between the coordination of Na compared with that of K and NH_4 . As a result, the crystal structure of malladrite Na_2SiF_6 (Zalkin *et al.*, 1964; Schäfer, 1986) is significantly different from those of K- or

TABLE 3. Crystal structure data of heklaite.

Orthorhombic $Pnma$

a 9.3387(7) Å
 b 5.5032(4) Å
 c 9.7957(8) Å
 V 503.43(7) Å³
 $Z = 4$

	x	y	z	B_{iso} (Å ²)
K	0.514(1)	¼	0.1785(7)	2.0(3)
Na	0.373(1)	¼	0.563(2)	2.2(3)
Si	0.227(1)	¼	0.924(2)	1.4(5)
F(1)	0.325(1)	0.472(3)	0.991(2)	3(1)
F(2)	0.133(1)	0.036(3)	0.858(1)	5(1)
F(3)	0.116(2)	¼	0.054(2)	5(1)
F(4)	0.341(2)	¼	0.788(2)	5(1)

NH_4 -compounds. The structure of heklaite differs significantly from all other silicofluorides, as we describe below.

In malladrite, F atoms form an hexagonal eutaxy (...ABAB...). In this arrangement, half the vacant octahedrally-coordinated XF_6 sites are

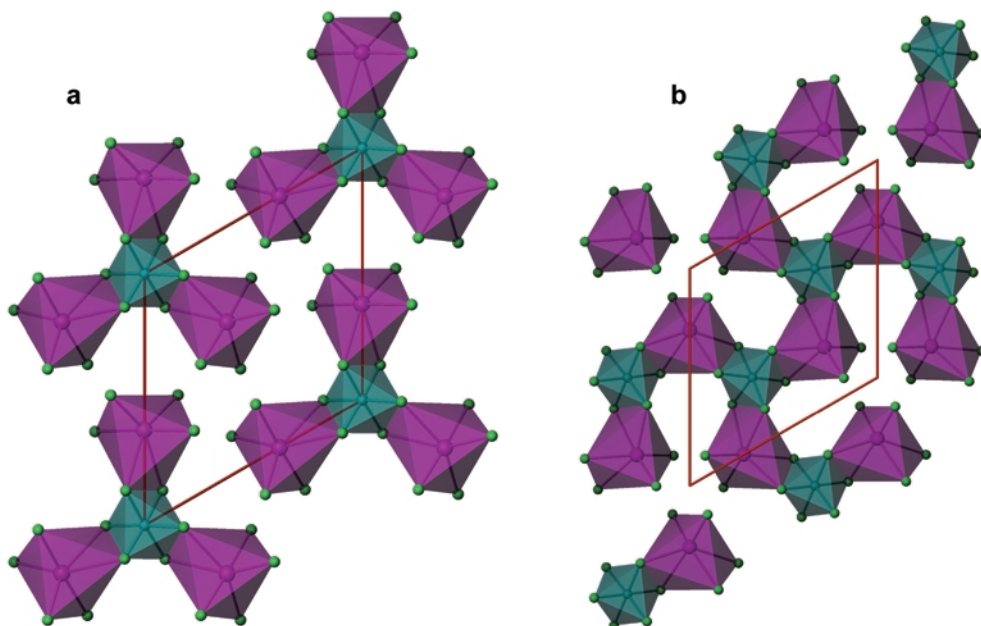


FIG. 4. The crystal structure of malladrite (Zalkin *et al.*, 1964; Schäfer, 1986) projected on (001). Two adjacent (001) layers are shown. The propeller groups of central SiF_6 octahedra (dark cyan) surrounded by three NaF_6 octahedra (magenta) form continuous upper layers with holes underlined by similar isolated propeller groups.

occupied in the ratio $1 \times \text{SiF}_6:2 \times \text{NaF}_6$. The crystal structure is shown in Fig. 4. Note that the empty octahedra in one layer overlie the occupied ones in the adjacent layer and that there are two types of cationic layers. In one layer (Fig. 4a), SiF_6 octahedra share edges with three NaF_6 octahedra which further interconnect them

to a two-dimensionally infinite slab. In the other layer (Fig. 4b), SiF_6 octahedra connected by edges to three surrounding NaF_6 octahedra appear again, but such propeller-like groups are isolated from each other in this layer and connect only to the coordination polyhedra from adjacent layers of the first type.

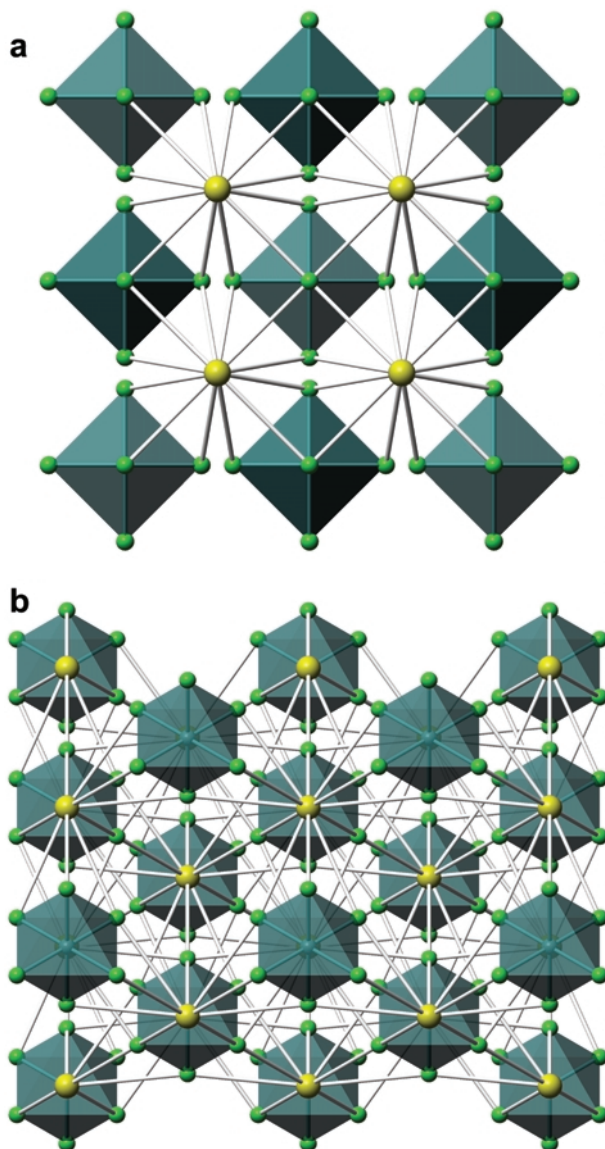


FIG. 5. The crystal structure of hieratite (Hester *et al.*, 1993). (a) View along $[100]$. (b) Projection onto (111) (only two layers with octahedra shown). SiF_6 octahedra (dark cyan) are surrounded by K atoms (yellow) in cuboctahedral coordination with F atoms (green).

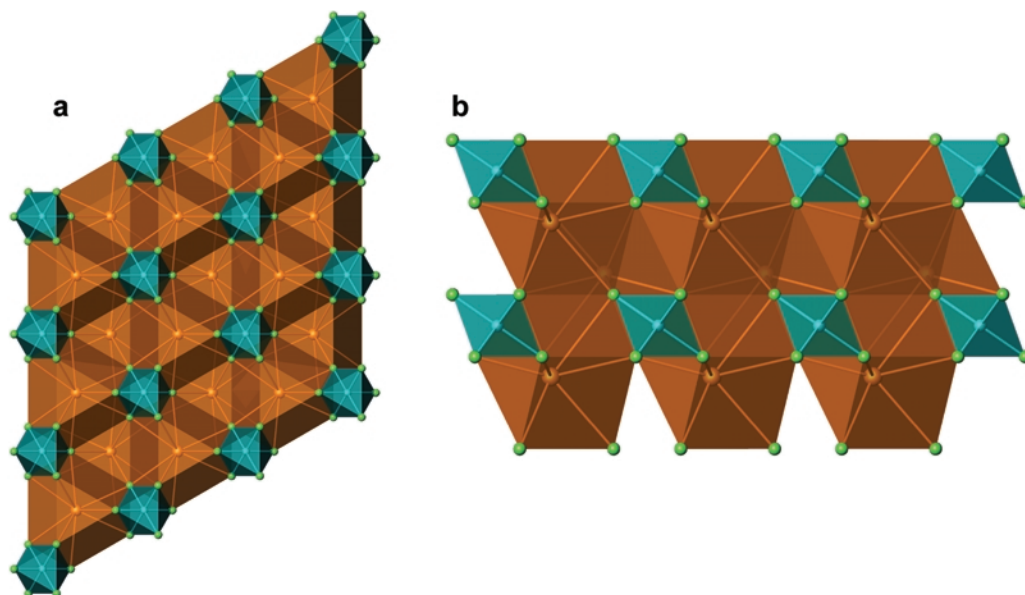


FIG. 6. The crystal structure of bararite (Gossner and Kraus, 1934). (a) Projection onto (001). (b) View along $[\bar{1}00]$. SiF_6 octahedra (dark cyan) are surrounded by NH_4 groups (in orange) in anticuboctahedral coordination with F atoms (green).

The structures of K- or NH_4 -silicofluorides are based on eutactic arrangements, where both F and K/ NH_4 partake and Si atoms fill isolated octahedral holes surrounded exclusively by F atoms. Potassium or NH_4 assume coordinations typical for atoms in eutaxies, either a cuboctahedron or a twinned cuboctahedron (anticuboctahedron). The sequence of eutactic layers, disregarding the differences between F and K/ NH_4 , is of a cubic-eutaxy type ($\dots\text{ABCABC}\dots$) in the K/ NH_4 isostructural pair hieratite/cryptohalite (Ketelaar, 1935; Hester *et al.*, 1993), of an hexagonal-eutaxy type ($\dots\text{ABAB}\dots$) in the $(\text{NH}_4)_2\text{SiF}_6$ polymorph bararite (Gossner and Kraus, 1934), and of a special $\dots\text{ABCBABC}\dots$ type in the K_2SiF_6 polytype demartinite (Gramaccioli and Campostrini, 2007) and hexagonal synthetic $(\text{NH}_4)_2\text{SiF}_6$ (Fábrý *et al.*, 2001). Cubic hieratite (Fig. 5) and cryptohalite belong to the K_2PtCl_6 structure type and are directly related topologically to perovskite, from which they differ in having half the octahedral sites empty, thereby isolating occupied octahedra from each other. The layer-to-layer sequence of occupied octahedra in bararite, $(\text{NH}_4)_2\text{SiF}_6$ (Fig. 6), leads to trigonal symmetry. In the case of demartinite and hexagonal synthetic $(\text{NH}_4)_2\text{SiF}_6$ (Fig. 7), K or NH_4 have two coordinations, a cuboctahedral one

similar to that in hieratite/cryptohalite and an anticuboctahedral one similar to that in bararite.

The structure of synthetic KNaSiF_6 (Fischer and Krämer, 1991), the synthetic analogue of heklaite, contains strips of octahedra and adjacent Na and K atoms which run parallel to the b axis (Fig. 8) and resemble those of hieratite. However, the eutactic arrangement of F and Na/K atoms is not present in this structure due to distortion around the K sites. It can be seen from Fig. 8a that K atoms do not fit in the same (100) layers with F atoms, whereas Na atoms are coplanar with F atoms. The strips of quasi-eutactic arrangement are displaced relative to their neighbours so that Na and K assume a 10-fold and 9-fold coordination respectively. It is a peculiarity of this structure that the cation with the shorter bond lengths has a larger coordination number (Fischer and Krämer, 1991).

Discussion

Heklaite, ideally KNaSiF_6 , belongs to the group of fluorosilicate minerals which form in F-rich fumarolic environments, such as the Hekla volcano.

The importance of fluorides such as HF and SiF_4 in mass transport during degassing processes

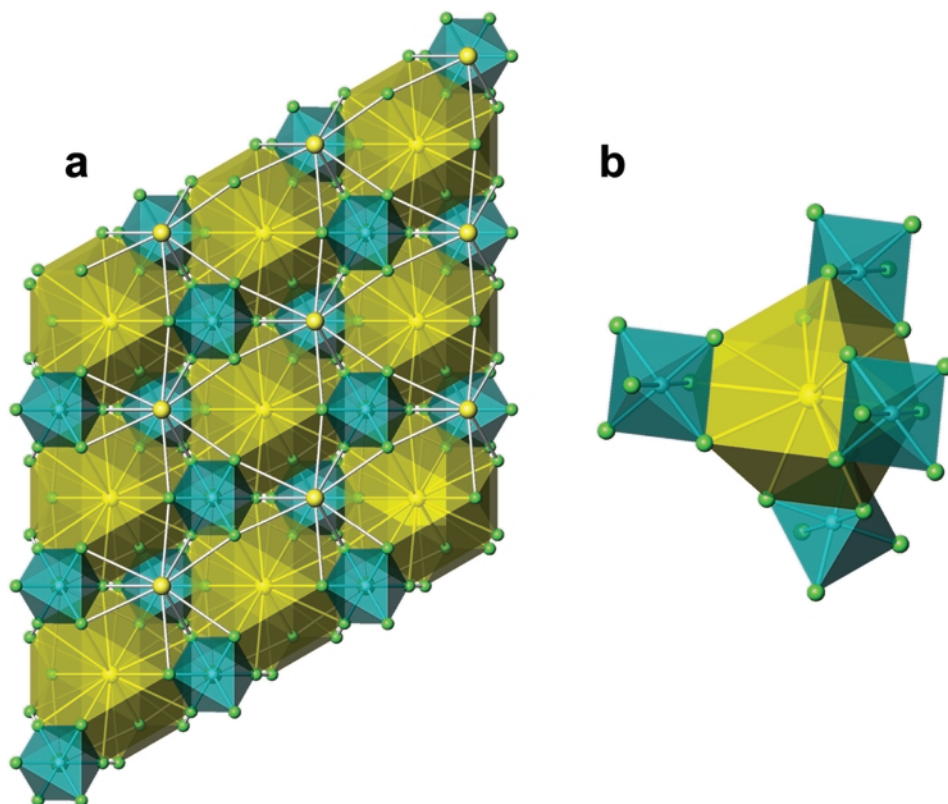
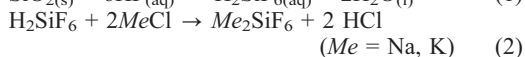


FIG. 7. The crystal structure of demartinite (Gramaccioli and Campostrini, 2007). SiF_6 octahedra (dark cyan) are surrounded by K atoms (yellow) of which one half are in cuboctahedral and the other half in anticuboctahedral coordination with F atoms (green). The cuboctahedral coordinations are indicated in (a), which is a projection onto (001). Details of the anticuboctahedral coordination are shown in (b).

was shown by White and Hochella (1992), who describe the depletion of weathering surfaces of lava flow in SiO_2 and enrichment in Ca, Al and Mg during post-eruptive degassing of cooling magma bodies. Thermodynamic calculations indicated that silica phases may form as a result of decompression of HF-rich gases rising to the surface, and also during heating of SiF_4 -bearing gases (De Hoog *et al.*, 2005). Hydrogen fluoride is the dominant F-bearing species in volcanic gases at $T > 400^\circ\text{C}$, whereas SiF_4 is the most abundant species at lower temperatures (Rosenberg, 1973).

The chemistry of the HF– SiO_2 system indicates that there is no reaction between HF and SiO_2 under dry conditions, and it is the excess of water in the volcanic gaseous steam that allows reaction to take place. Reaction is also favoured by the simultaneous presence in the steam of

strong acids (e.g. HCl). Possible reactions explaining the formation of heklaite in cooling F-rich volcanic gases are:



The orthorhombic crystal structure of KNaSiF_6 differs from both cubic and hexagonal K_2SiF_6 and (pseudo)trigonal Na_2SiF_6 . Potassium and Na occupy distinct positions in heklaite and have different coordination numbers. It is, therefore, unlikely that significant solid solutions exist between KNaSiF_6 and other end members in the Na_2SiF_6 – K_2SiF_6 system. Consequently, the mineral associations would change from $\text{Na}_2\text{SiF}_6 + \text{KNaSiF}_6$ to $\text{K}_2\text{SiF}_6 + \text{KNaSiF}_6$ with a varying Na:K ratio in the gas phase. This

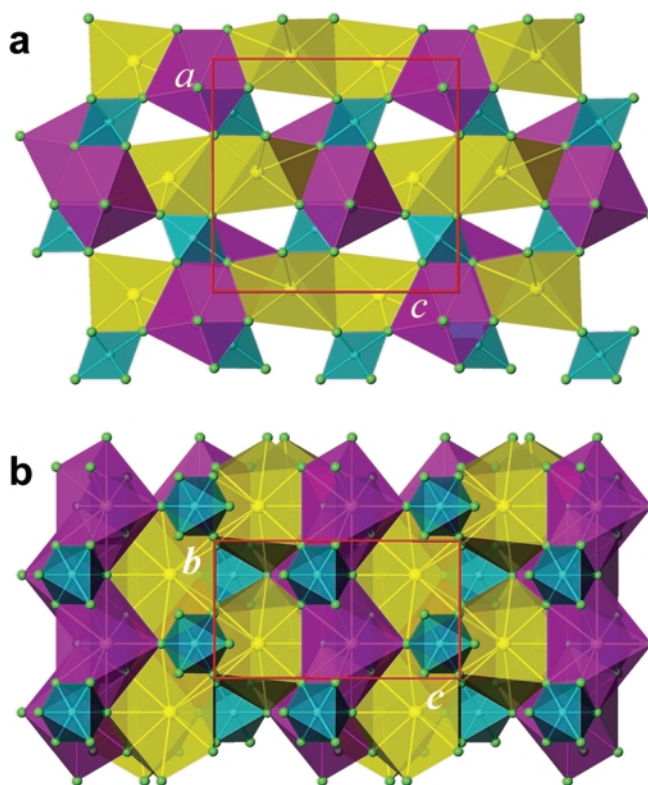


FIG. 8. The crystal structure of heklaite. SiF₆ octahedra are in dark cyan colour, K coordination yellow and Na coordination magenta. (a) Projected onto (010). (b) Projected onto (100). For structural details see text.

inference suggests that heklaite should be a common fumarolic phase accompanying mallardrite or K₂SiF₆ polymorphs, if both Na and K are present in significant quantities. The coexistence of all these silicofluorides in Hekla encrustations indicates non-equilibrium deposition from a gaseous steam which changed composition very quickly and contained approximately equal amounts of Na and K.

Reactions 1 and 2, proposed to explain heklaite formation in fumarolic environments, correspond to normal laboratory procedures for the synthesis of fluosilicate compounds, which use metal chloride solution and fluosilicic acid. In these laboratory conditions, the crystallization of the synthetic materials is very rapid, and the deposition occurs immediately on mixing the reactants. Rapid crystallization is consistent with the minute size of crystals of natural heklaite, whose deposition must be very rapid and under non-equilibrium conditions.

Acknowledgements

Sigurdur S. Jonsson, at the Iceland GeoSurvey, Reykjavik, is thanked for assisting in collecting encrustations at Hekla. The authors are grateful to Tove Fredslund and Helene Almind for their help in the preparation and XRD measurements of samples. The help of the editor Dr Mark Welch and of the reviewer Dr Elena Sokolova in improving the text and figures is highly appreciated. This work was financially helped by NordForsk through Nordic Mineralogical Network and by the Danish National Research Council.

References

- Acquafredda, P. and Paglionico, A. (2004) SEM-EDS microanalyses of micropheocrysts of Mediterranean obsidians: a preliminary approach to source discrimination. *European Journal of Mineralogy*, **16**, 419–429.

HEKLAITE, KNaSiF_6 , A NEW FUMAROLIC MINERAL FROM HEKLA VOLCANO, ICELAND

- De Hoog, J.C.M., Van Bergen, M.J. and Jacobs, M.H.G. (2005) Vapour-phase crystallisation of silica -from SiF_4 -bearing volcanic gases. *Annals of Geophysics*, **48**, 775–785.
- Fábry, J., Chval, J. and Petříček, V. (2001) A new modification of diammonium hexafluorosilicate, $(\text{NH}_4)_2[\text{SiF}_6]$. *Acta Crystallographica E*, **57**, 90–91.
- Fischer, J. and Krämer, V. (1991) Crystal structure of KNaSiF_6 . *Materials Research Bulletin*, **26**, 925–930.
- Gossner, B. and Kraus, O. (1934) Das Kristallgitter von Ammoniumhexafluorosilikat $(\text{NH}_4)_2\text{SiF}_6$. *Zeitschrift für Kristallographie*, **88**, 223–225.
- Gramaccioli, C.M. and Camprostrini, I. (2007) Demartinite, a new polymorph of K_2SiF_6 from La Fossa crater, Vulcano, Aeolian Islands, Italy. *The Canadian Mineralogist*, **45**, 1275–1280.
- Gudmundsson, A., Oskarsson, N., Grönvold, K., Saemundsson, K., Sigurdsson, O., Stefansson, R., Gislason, S.R., Einarsson, P., Brandsdóttir, B., Larsen, G., Johannesson, H. and Thordarson, Th. (1992) The 1991 eruption of Hekla, Iceland. *Bulletin of Volcanology*, **54**, 238–246.
- Hester, J.R., Maslen, E.N. and Spadaccini, N. (1993) Accurate synchrotron radiation $\Delta\rho$ maps for K_2SiF_6 and K_2PdCl_6 . *Acta Crystallographica B*, **49**, 967–973.
- Jakobsson, S.P., Jonasson, K. and Sigurdsson, I.A. (2008a) The three igneous rock series of Iceland. *Jökull*, **58**, 117–138.
- Jakobsson, S.P., Leonardsen, E., Balić-Žunić, T. and Jónsson, S.S. (2008b) Encrustations from three recent volcanic eruptions in Iceland: The 1963–1967 Surtsey, the 1973 Eldfell and the 1991 Hekla eruptions. *Fjölrit Náttúrufræðistofnunar*, **52**, 65 pp.
- Ketelaar, J.A.A. (1935) Die Kristallstruktur von K-, Rb-, Cs- und Tl-Silicofluorid und von $\text{LiMnO}_4 \cdot 3\text{H}_2\text{O}$. *Zeitschrift für Kristallographie*, **92**, 155–156.
- Rosenberg, P.E. (1973) HF/ SiF_4 ratios in volcanic and magmatic gases. *Geochimica et Cosmochimica Acta*, **37**, 109–112.
- Ruste, J. (1979) X-ray spectrometry. Pp. 215–267 in: *Microanalysis and Scanning Electron Microscopy* (F. Maurice, L. Meny and R. Tixier, editors). Les Editions de Physique, Orsay, France.
- Schäfer, G.F. (1986) The crystal structures of Na_2TiF_6 and Na_2SiF_6 . *Zeitschrift für Kristallographie*, **175**, 269–276.
- White, A.F. and Hochella, M.F. Jr (1992) Surface chemistry associated with the cooling and subaerial weathering of recent basalt flows. *Geochimica et Cosmochimica Acta*, **56**, 3711–3721.
- Zalkin, A., Forrester, J.D. and Tempelton, D.H. (1964) The crystal structure of sodium fluosilicate. *Acta Crystallographica*, **17**, 1408–1412.

